Proceedings of the ICBBG2025
2025 International conference on Bio-mediated and Bio-inspired Geotechnics
18-20 May, 2025 | Tempe, Arizona, USA
https://doi.org/10.53243/ICBBG2025-181

Durability of Biocalcified Porous Materials Exposed to Solutions of Varying Aggressiveness: Model-Based Measurements and Short- and Long-Term Issues

Lorenzo Spadini,[1] Laurent Oxarango,[1] Emilie François,[1]
Leslie Sapin,[2] Annette Esnault Filet,[2] Jean M.F. Martins[1]

[1]IGE UMR 5001 / UGA / CNRS / G-INP/ IRD, 38041 Grenoble, France; E-mail: lorenzo.spadini@univ-grenoble-alpes.fr, jean.martins@univ-grenoble-alpes.fr, laurent.oxarango@univ-grenoble-alpes.fr
[2]Soletanche-Bachy, 280 avenue Napoléon Bonaparte , 92300 Rueil Malmaison , France; E-mail: leslie.sapin@soletanche-bachy.com, Annette.esnault@soletanche-bachy.com

ABSTRACT

Controlled biocalcification is an emerging way to increase the mechanical cohesion of granular materials through the formation of grain-bridging concretions. However, this increase in cohesion can be lost through chemical dissolution and/or mechanical stress on the long term. This study investigates the evolution of the cohesion of porous materials biocalcified by *Sporosarcina pasteurii* under controlled conditions in columns. Experimental and theoretical leaching tests conducted with pure water alone led to horizontal dissolution profiles, i.e. dissolution of calcite only at the point of entry into the column. Conversely, leaching in presence of Tris-hydroxy-methyl-aminomethane (TRIS) generated subvertical dissolution profiles. The slightly acidic pH of the optimized TRIS solution and its moderate complexing strength increase the solubility of calcite. This increases the dissolution time and therefore allows calcite to be dissolved over a larger section and length of the column. Thermodynamic modelling made it possible to decipher the dissolution mechanisms and to predict the dissolution patterns in various realistic situations.

INTRODUCTION

Biocalcification is a microbially induced carbonate precipitation process that can potentially and sustainably improve soil's resistance. Biocalcification permits to stabilize porous materials by in-pore precipitation of carbonate produced locally by the hydrolysis reaction of urea by injected microorganisms with Ca^{2+}, leading to pore-filling and grains fixing through bridges formation [1,2].

This recent technology can possibly be more environment friendly than conventional chemical and mechanical methods and is now being applied to various objects such as granular embankments, dikes, buildings and work of art. Calcite is the pore-filling material, and this solid is known to dissolve in presence of acids. Acidifying processes such as soil respiration, infiltration of acidic waters into porous matrices etc. can therefore affect the stability of biocalcified materials through the export of cementing calcite by dissolution. In this study, the durability of biocalcified sandy columns is determined by injection of an aggressive solution. Interpretation of specifically designed experimental together with geochemical modelling reveals the mechanisms involved in

dissolution and allows conclusions to be drawn about the durability of biocalcified materials in different real environments.

MATERIAL AND METHODS

Calcite dissolution and precipitation.

Calcite solubility at chemical equilibrium: Calcite saturation state and dissolution kinetics are presented in an interpretative manner for the purposes of understanding this study.

In a closed system (a closed reactor exchanging neither materials nor energy with the 'outer' space, e.g. the outer atmosphere), at circumneutral pH, the calcite dissolution-precipitation reaction of calcite determining its solubility is as follows:

$$CaCO_{3(s)} + H^+ \rightarrow Ca^{+2} + HCO_3^- \; ; \log K_s \quad (1)$$

or respectively

$$K_s = (Ca^{+2})(HCO_3^-)(H^+)^{-1}; \text{ s for 'solid'} \quad (2)$$

with K_s representing the solubility constant of calcite, and $LogK_s$ its decimal logarithm. Solubility constants are threshold values: the activity products measured (e.g. $(Ca^{+2})(HCO_3^-)(H^+)^{-1}$ in Equation (2)), which are equal to, less than or greater than K_s represents an assembly of ions, which are saturated, undersaturated or oversaturated with respect to the associated solid (calcite in this case). The term (i^{+z}) represents the activity of the ion i charged z^+.

In such a closed system, the two products Ca^{+2} and HCO_3^- are supplied by calcite alone, which implies in a pure calcite-water system the fixed stoichiometric relationship $[Ca^{+2}]\sim[HCO_3^-]$, Equation (2) simplifying to ($[i^{+z}]$ the concentration of i)

$$K_s \cdot (H^+) \sim (Ca^{+2})^2 \quad (3)$$

This reaction highlights the strong increase in the solubility of calcite as the pH decreases. The formation of hydrolysis products of $Ca(OH)_x^{2-x}$ as a function of pH and the deprotonation of HCO_3^- to CO_3^{-2} attenuate the solubility decrease. The solubilities of calcite in a system of closed pure water at pH 9.9, 8.3, 7, 6 calculated with PHREEQC geochemical code are 0.12, 0.69, 3.9, 25 mmol/L [3,4].

Acid consumption in a closed system of pure calcite-water results in a basic equilibrium pH of 9.9. Calcite solubility is therefore low (0.12 mmol/L). The addition of acid causes the equilibrium pH towards move to lower values, i.e. towards higher calcite solubilities.

In a reactor open to the atmosphere the base produced by the dissolution of calcite is neutralized by atmospheric carbon dioxide:

$$CaCO_{3(s)} + CO_{2(g)} + H_2O \rightarrow Ca^{+2} + 2\,HCO_3^- \; ; \log K_{s'} \quad (4)$$

In such a system the solubility of calcite essentially depends on the CO_2 partial pressure pCO_2. The products Ca^{+2} and HCO_3^- are supplied by Calcite and $CO_{2(g)}$ alone, implying the fixed

concentration relationship $2[Ca^{+2}] \sim [HCO_3^-]$ on the product side, and hence the possible simplification of the corresponding solubility equation

$$K_s' = (Ca^{+2})(HCO_3^-)^2 / pCO_2 \quad (5)$$

to

$$K_s' \sim (Ca^{+2})\{2(Ca^{+2})\}^2 / pCO_2 = 4\,(Ca^{+2})^3 \quad (6)$$

In this situation, the equilibrium pH is buffered and controlled by the pCO_2. The equilibrium pH and Ca concentration of pure water in contact with calcite at the atmospheric $pCO_{2(atm.)}$ of $10^{-3.5}$ atm. are respectively 8.3 and 0.49 mmol/L or 20 mg/L Ca^{+2}. Due to subsoil respiration continental waters (common river, lake and groundwaters) have pCO_2 up to two orders of magnitude the atmospheric one [3]. At pCO_2 of $10^{-2.5}$ and $10^{-1.5}$ atm. pH and $[Ca^{+2}]$ are respectively 7.6 and 44 mg/L, and 7.0 and 100 mg/L. These values correspond to those found in common continental waters, e.g. groundwaters and with it bottled mineral waters, tap-, river- and groundwaters. It should be noted that in pure water-calcite systems open to the atmosphere the four parameters pH, (Ca^{+2}), (HCO_3^-) and pCO_2 are closely linked, with the fixation of one of these four variables fixing the three other values.

Calcite dissolution kinetics: The dissolution kinetics of solid calcite depend on pH, pCO_2 and calcite surface area. Above pH 5 and up to Log pCO_2 < -0.96 atm., which is ~347 times the $pCO_{2(atm.)}$, the dissolution rate of calcite is constant ($r_3 = k_3 = 10^{-9.93}$ mol cm^{-2} s^{-1}, figure 1). At higher pCO_2 and above pH 5, the overall rate is always constant but higher and linearly correlated to pCO_2: $r_2=(H_2CO_3)\cdot k_2= K_H\cdot pCO_2\cdot k_2$; $k_2 = 10^{-7.47}$ cm s^{-1}; K_H(25 °C, 1 bar)=$10^{-1.5}$ mol L^{-1} $atm.^{-1}$ the Henri factor). Such high pCO_2 are not common in soil and groundwater. Finally, below pH 5 the dominant mechanism is strongly pH-dependent: ($r_1 = (H^+)\cdot k_1$; $k_1 = 10^{-4.29}$ cm s^{-1}) relating to the known acid sensitivity of carbonated rocks.

The generic rate expression is the sum of the three mechanisms, as follows:

$$r_{dis} = r_1 + r_2 + r_3 = k_1 \cdot (H^+) + k_2 \cdot (H_2CO_3) + k_3 \quad (7)$$

generating the overall dissolution rate r_{dis} presented in figure 1 [5,6].
The maximum solubility at minimum dissolution rate is at pH 6. This pH represents the breakpoint of small *versus* high dissolution rate at minimum pH, i.e. at maximum calcite solubility. This represents the optimum working pH for our experiments.

Preparation of the aggressive solution.

Acid addition shifts the pure water – calcite equilibrium pH from 9.9 to lower values. Evaluated candidates such as imidazole (pK=7.0) or picolinic acid (pK=5.5) were abandoned due to toxicity or chemical stability considerations. An additional constraint is the necessary low complexation strength of the final candidate to avoid active extrusion of Ca^{+2} ions from the calcite surface, which may unrealistically increase the dissolution rate. The finally chosen substance Tris (tris(hydroxymethyl)aminomethane) has a pKa value somewhat higher (pK 8.1) than the 'ideal' one (~ 6). The used composition of the aggressive solution was a buffering mixture of 195 mmol/L

$HTRIS^+$ (added as Cl^- salt) and 5 mmol/L TRIS. The excess concentration of the acidic form decreased the equilibrium pH to 7.0. At this pH the theoretical $[Ca^{+2}]$ solubility is 3.9 mmol/L instead of 25 mmol/L at the 'ideal' pH of 6 (closed system). This working solution is further referenced as 'TRIS solution'.

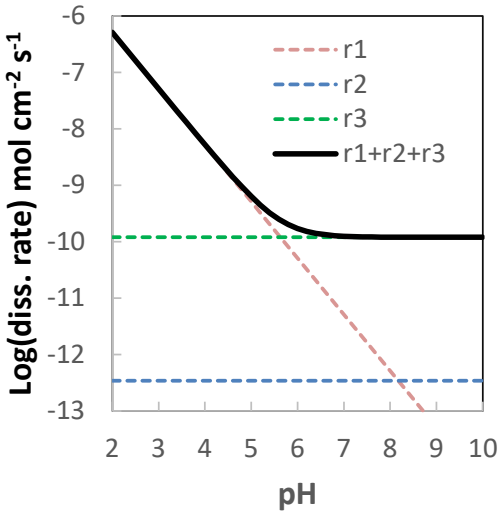

Figure 1. Dissolution kinetics of Calcite. In the figure the rate r_2 is levelled at $pCO_{2(atm.)}$

Materials, reactive transfer conditions and analysis.

The base material used is the Fontainebleau sand (grain size 230µm, d_{50} = 120µm) biocalcified with *S. pasteurii*. The biocalcification procedure is presented in [7]. From the obtained biocalcified sandy blocks, some columns were carved for the durability tests. The initial concentrations inside the used calcite column are considered equal to the mean concentration of calcite determined around the cavity of the extracted column. From this, an initially homogeneous distribution of calcite inside the column is implicitly assumed.

At the end of column leaching experiments the columns were destructively cut into seven slices, and each slice was separately analysed for solid calcite.

The 7 cm long, 3.5 cm diameter biocalcified columns were packed and encased in waterproof fabric. The columns were initially water saturated by slowly injecting specific commercially available mineral water from bottom to top, to prevent air trapping ('Cristaline' brand, St. Sophie source, pH 7.4). Porosity was determined by weighting empty *versus* water saturated columns in all experiments. Then, the aggressive TRIS solution was injected. At the end, the mineral water was again injected during the time necessary to drive the CE values down to 800 µS/cm. Three duplicated experiments varying in flow rate are presented. Continuous measurement of the electrical conductivity (CE) at the outflow was assessed with a CE flow-through cell connected to an Agilent relay itself connected to a recorder PC (Agilent software interface).

Solid calcite and dissolved calcium were measured respectively with a Bernard Calcimeter (IGE Laboratory) and by ICP-AES (Varian 720ES, ISTERRE Laboratory, Grenoble). Scanning electron microscopy images were obtained at the 'consortium des moyens technologiques communs' (MEB-FEG Ultra 55 ZEISS with X-ray microprobe, CMTC laboratory, Grenoble). Table 1 provides additional column-specific information.

Table 1. Column-specific experimental conditions and results.

Essai	Initial calcite mass % [a]	Darcian flow cm/h	Injected volume of TRIS solution	pH [b]	EC [b] [mS/cm]	Dissolved calcite: mass% [a]; mass%/PV [c]
ED1	3,1 ± 0,1 %	3	2,6 L, 129 PV	7.0	15	1,25 % ; 0.0097 %
ED2	3,6 ± 0,1 %		3,9 L, 193 PV	7.2	16	1,90 % ; 0.0097 %
ED3	3,5 ± 0,1 %	27	4,0 L, 198 PV	7.0	14.5	1,90 % ; 0,0096 %
ED4	2,6 ± 0,2 %		3,9 L, 193 PV	7.25	15.5	1,70 % ; 0,0090 %
ED5	3,8 ± 0,1 %	120	5,9 L, 292 PV	6.9	15.9	2,70 % ; 0,0092 %
ED6	3,3 ± 0,1 %		5,8 L, 287 PV	7.1	14.5	2,60 % ; 0,0090 %

a) % mass of calcite normalized toward total dry solid mass (sand plus calcite). b) Average plateau values. c) % mass of calcite divided the pore volume.

Geochemical Modelling.

Modelling was assessed with the PHREEQC geochemical code [3]. Fitting was performed by visually recover experimental and modelled data as the code does not include automated difference minimization procedures. Reactive transfer experiments are assessed by slicing the 7 cm long columns in 14 stacked model reactors of 0.5 cm length each, in which instantaneous equilibration of all reactions is assumed except those explicitly defined as time-dependent. A shift represents the transfer of the solutes from cell n to cell n+1 along the column, one pore volume (PV) is consequently exchanged after 14 shifts. The PHREEQC scripts may be delivered on request.

RESULTS

Reactive transfer experiments.

Figure 2 (a, c) shows that not vertical, but subvertical dissolution profiles were obtained whatever the flow rate applied, with more calcite exported in the high flow experiments as more aggressive solution was transferred. At the outlet of the column pH and CE stabilized rapidly to constant values, which were almost same for all experiments whatever the flow rate applied (Figure 2 b,d and table 1). In particular, a unique value is obtained for the mass of dissolved calcite divided by the pore volumes of injected aggressive TRIS solution.

This means that the exported mass of calcite does not depend on the flow rate despite the strong variation of this parameter between experiments. This evidences that the dissolution of calcite is controlled not from calcite dissolution kinetics but from chemical equilibrium, with calcite at saturation state at the column outlet. Concordantly, the amount of solid calcite dissolved at the column outlet is null or almost null inferring a calcite saturation state of the percolating solution at that depth. The discrepancies measured between initial and final calcite concentrations at the column outlet, as observed for example in figure 2a (red lines), are potentially due to the simplifying assumption of homogeneous calcification profiles along the column.

Data modelling.

Good agreement was obtained between modelled and experimental data for (a) the rapid increase followed by stabilization over time in pH and EC, with particularly good pH reproducibility (table 2 compared with table 1). At the column inlet, all modelled calcite is completely dissolved, in

contrast to the column outlet, where no or almost no calcite (fast flow) has been dissolved (figure 3 and table 2). At the same time, the modelled saturation index is zero (almost zero for maximum flow experiments) at the column outlet (table 2). This means that calcite saturation is reached at the column outlet. Consequently, and naturally, the percentage of total modelled calcite mass exported divided by pore volume is also constant at all flow rates.

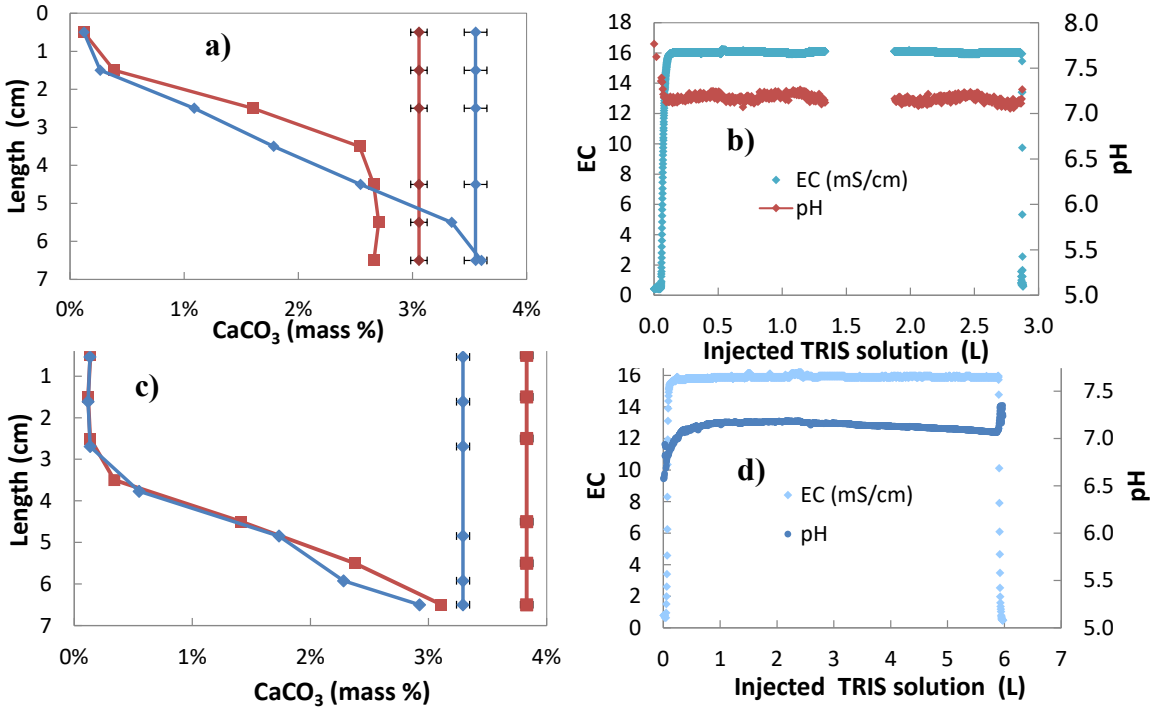

Figure 2. a,c: Measured mass of solid calcite present in the columns before (vertical profiles) and after (curved profiles) flushing the columns with the aggressive TRIS solution at the minimum (a, 0.6 ml/min., ED1, ED2) and maximum (c, 19 ml/min., ED5, ED6) flow rates. a and b represents duplicated experiments in blue and red. b,d: EC and pH measurements at the column outlet of one of the replicates at minimum (b) and maximum (d) flow rates.

Experiments and modelling lead to a clear and obvious interpretation: calcite dissolution kinetics operate *inside* the column but are so rapid that chemical equilibrium is reached at the *outlet* of the columns, which are only 7 cm long. This underlines the speed of dissolution kinetics, which will be important for the durability of calcified structures.

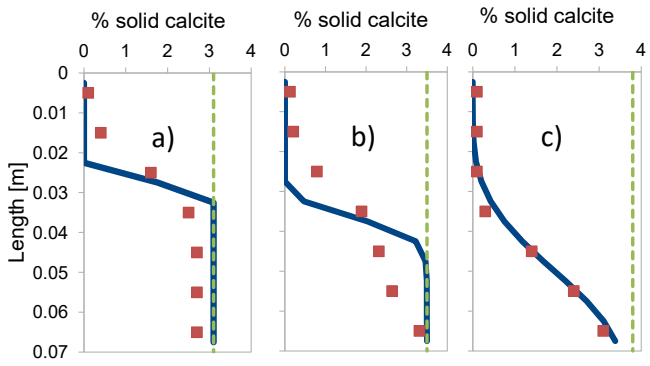

Figure 3. Final experimental (red squares), final modelled (blue lines), and initial homogenized experimental (green line) % solid calcite profiles of the minimum (a, ED1), intermediate (b, ED3) and maximum (c, ED6) flow rate experiments. Solution entrance is at the column top.

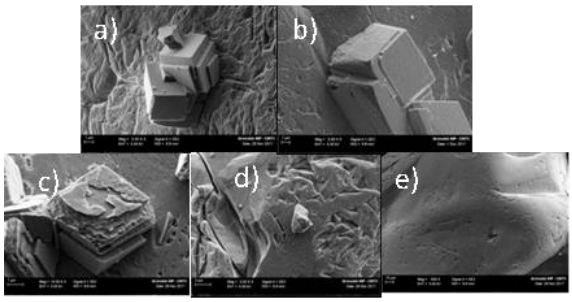

Figure 4. SEM images of bio-precipitated calcite in its initial state (a,b), leached with the TRIS solution (c,d), and entirely dissolved after prolonged exposure (e).

In modelling, the specific surface area is the only parameter adjusted. The applied value of 1 m^2 g^{-1} is in good agreement with calculations based on 3D X-ray tomography studies [8]. Separate leaching experiments show that initially regular cementing calcite grains develop kinks and edges while decreasing in size before being completely dissolved (figure 4). More specifically, good agreement between measured and modelled final calcite mass profiles is only obtained for the maximum flow measurement (figure 3c). As expected, in modelling the profiles are more staircase-shaped at the lower the flow rates. But the measured data do not follow this trend, with rather regular profiles with steep slopes being recorded at all flow rates. They are simply shifted downwards for experiments at higher flow rates as a function of the greater volume of aggressive solution injected (figure 3 a versus c). Two processes are discussed below: (1) during calcite dissolution, pCO_2 increases inside the column, representing a semi-closed system. The pCO_2 could exceed the threshold value of Log pCO_2 = 0.96 atm., leading to an increase in dissolution kinetics. But the pCO_2 values modelled are below this value (table 2), and increasing dissolution rates at constant flow rates should favour “staircase” profiles - yet the opposite is observed.

A better hypothesis is the possible diffusion-controlled dissolution process: a local concentration of dissolved calcite around the grains might inhibit dissolution, particularly in calcite-undersaturated zones. This process would increase the slope of solid calcite along the column especially in low-flow experiments, making them resemble *in fine* the slopes observed in high-flow experiments. This process is currently not included in the model.

Table 2. Modelling results obtained for the last shift (at the end) of TRIS solution injection.

	pH [a]	[Ca_{aq}] [a] mmol/L	Calcite [a] mass%	DisCalcite [b] mass% / PV	Sat.index [a]	EC [a] mS/cm	Log(pCO_2)[a]
ED1	6.7, 7.0	0.25, 6.0	0.0, 3.1	0.0093	-3.2, 0.0	12.2, 12.8	-2.7, -1.6
ED2	6.7, 7.0	0.29, 6.0	0.0, 3.6	0.0093	-3.0, 0.0	12.2, 12.8	-2.6, -1.6
ED3	6.7, 7.0	0.28, 6.0	0.0, 3.5	0.0093	-3.1, 0.0	12.2, 12.8	-2.6, -1.6
ED4	6.7, 7.0	0.21, 6.0	0.0, 2.6	0.0093	-3.3, 0.0	12.2, 12.8	-2.7, -1.6
ED5	6.7, 7.0	0.30, 5.5	0.0, 3.4	0.0091	-3.0, -0.1	12.2, 12.7	-2.6, -1.6
ED6	6.7, 7.0	0.27, 4.8	0.0, 2.5	0.0090	-3.1, -0.2	12.2, 12.6	-2.6, -1.6

a) Model values of the 1st (column inlet) and the last 14th (column outlet) model slice.
b) Whole column (sum of the 14 slices) % mass of dissolved calcite divided the pore volume.

Implications for biocalcified structures.

The implications for biocalcified structures are as follows: continental waters saturated or oversaturated with calcite do not dissolve bioprecipitated calcite, i.e. they do not affect their mechanical stability over time. The opposite applies to calcite-undersaturated waters. In this situation, the loss of biocalcified material is rapid and destructive in terms of material cohesion. The mass of solid bio-cement lost in solution depends solely on (a) the state of calcite undersaturation, which can be easily assessed from basic measurements of three aqueous parameters (pH, [Ca^{+2}] and alkalinity = [HCO_3^-]), and (b) the water flow. In practice, the installation of biocalcified structures should be avoided in "crystalline" geological environments (e.g. streams flowing exclusively in granitic environments) and in other low pH, calcite-undersaturated waters (e.g. streams downstream of sulfide-based mines undergoing acid mine drainage). Fortunately, most major rivers flow through concomitant carbonate and crystalline sedimentary environments, ensuring an aquifer composition that implies the presence of carbonate rocks. Therefore, calcite saturation - or even supersaturation- can be achieved. Continental waters are globally "protected" from a state of calcite undersaturation, since the subsurface pCO_2 exceeds atmospheric pCO_2 by one to two orders of magnitude [4]. The outgassing of CO_2 raises the pH, which in turn reduces the solubility of calcite and causes it to precipitate, thus protecting the biocalcified structure.

$$HCO_3^- + H^+ \Rightarrow H_2CO_3 \Rightarrow CO_{2(g)} + H_2O \quad (8)$$

The same process is responsible for the encrustation of household appliances such as washing machines, coffee machines, etc., except that the outgassing is triggered by the heating of the water.

The effect of organic matter (OM) depends on the context. In principle, respiration creates carbonic acid, which dissolves calcite and increases pCO_2. Biocalcified structures in contact with OM will therefore be weakened. Conversely, if water degassing at high pCO_2 and high Ca comes into contact with a biocalcified structure, calcite will precipitate, potentially protecting the structures. Biocalcified structures exposed to air are subject to dissolution by rainwater. Rainwater can be equated with pure water in an open system at $pCO_{2(atm.)}$, calcite solubility is at the values given above, pH will be 5.7 for "clean" rainwater, and correspondingly, pH will be lower and calcite solubility higher for acid rain. As a result, rainwater will weaken exposed biocalcified structures, all the more so as plant cover promotes respiration, i.e. high pCO_2 values in the root zone in contact with the biocalcified structure. Degradation of 500-year-old limestone buildings,

stones etc. by rainwater can be routinely observed. Biocalcified structures will be degraded much more rapidly, since (1) the calcite content is low and (2) the matrix is highly permeable.

CONCLUSION

The durability of biocalcified structures depends on the export of cementing precipitated calcite by dissolution. In the system studied, dissolution kinetics are very rapid, calcite dissolves rapidly up to the equilibrium concentration of calcite saturation. Consequently, the amount of calcite dissolved and the associated time are a function of just two parameters, namely the degree of calcite undersaturation and the flow rate. Biocalcified structures in contact with saturated / undersaturated water will not / will be strongly weakened. The installation of biocalcified structures in acidic waters, for example in crystalline geological environments, is not viable, nor will structures exposed to rainwater be weakened over short periods. Conversely, carbonated waters, which include most major rivers, can be considered "safe" due to the excess pCO_2 pressure of water over air, which ensures that saturated, or even supersaturated, conditions are maintained with regard to calcite solubility.

ACKNOWLEDGMENTS

The authors would like to acknowledge the FUI 16 of the French Government for the BOREAL project funding. Special thanks are due to E. Vince for technical help conducted within the technical AirOSol platform of IGE, which is part of the REGEF BGE Research Infrastructure of INSU CNRS. This work was supported by the Labex OSUG@2020, ANR grant #ANR-10-LABX-56 (funded by the Future Investments Program (PIA) launched by the French government and implemented by the French agency ANR.

REFERENCES

1. Suresh, D., and Uday, K. V. A. (2023). "Comparative Study of Various Parameters Influencing Biocalcification via Ureolysis Mediated by Enzyme and Microbe: A Comprehensive Review." *Geomicrobiology Journal*, 41(1), 17–34. https://doi.org/10.1080/01490451.2023.2283419
2. Beguin R., L. Oxarango, L. Sapin, A. Garandet, A. Viglino, E. Franoçis, H. Mora, J.M.F. Martins, L. Duchesne, D. Albrecht, A. Esnault-Filet, I. Gutjahr, L. Lépine. Experimental Tests of Soil Reinforcement Against Erosion and Liquefaction by Microbially Induced Carbonate Precipitation. Proceedings of EWG-IE 26th Annual Meeting 2018. Bonelli S., Jommi C., Sterpi D. (Eds). Chapter Internal Erosion in Earthdams, Dikes and Levees. DOI:10.1007/978-3-319-99423-9_2. September 2019.
3. Parkhurst D. L, and Appelo C. A. J. (2013). "PHREEQC version 3 - A computer program for speciation, batch-reaction, one-dimensional transport, and inverse geochemical calculations." U.S. Geological Survey. https://www.usgs.gov/software/phreeqc-version-3
4. Appelo, C.A.J., Postma D. (2005). "Geochemistry, Groundwater and pollution." Chapter 5. 2nd edn., eds. CRC press, London
5. Plummer L., Wigley T., Parkhurst D. (1978) "The kinetics of calcite dissolution in CO_2-water systems at 5°C to 60°C and 0.0 to 1.0 atm CO_2." *American Journal of Science* 278, 179-216. 10.2475/ajs.278.2.179

6. Wollast, R. (1990). “Rate and Mechanism of Dissolution of Carbonates in the System $CaCO_3$-$MgCO_3$.” in *Aquatic chemical kinetics: reaction rates of processes in natural waters*, Stumm, W., eds.Wiley, New York
7. Dadda A, Geindreau C., Emeriault F., Rolland du Roscoat S., Garandet A., Sapin L. and Esnault Filet A. (2017). “Characterization of microstructural and physical properties changes in biocemented sand using 3D X-ray microtomography.” *Acta Geotech*. 12, 955–970. https://doi.org/10.1007/s11440-017-0578-5
8. Geindreau C., Emeriault F., Abdelali Dadda A., Yaba O., Spadin L., Esnault Filet A., Garandet A. (2022). “Mechanical and Microstructural Changes of Biocemented Sand Subjected to an Acid Solution.” *Int. J. Geomechanics,* 22(3). https://doi.org/10.1061/(ASCE)GM.1943-5622.0002302